C.P. No. 954

C.P. No. 954

MINISTRY OF TECHNOLOGY

AERONAUTICAL RESEARCH COUNCIL

CURRENT PAPERS

Measurements of Wing Buffeting on a Scimitar Model

by

D. G. Mabey, M.Sc.(Eng.)

LONDON: HER MAJESTY'S STATIONERY OFFICE

1967

FIVE SHILLINGS NET

U.D.C. No. 533.6.013.43 : 533.693

C.P. No.954*
May 1966

MEASUREMENTS OF WING BUFFETING ON A SCIMITAR MODEL

by

D. G. Mabey, M.Sc. (Eng.)

SUMMARY

Measurements of unsteady wing-root strain were made on a small solid model of the Scimitar Mk.1 aircraft to investigate the buffeting scaling relationships. The wing-root strain measurements covered an incidence range from 0° to 13° at a Mach number of 0.50 and a wide range of stream density.

The derived buffeting scaling relationships show that the damping of the wing buffeting is predominantly structural (even though the structural damping coefficient on this model is low) because the aerodynamic damping coefficient is low owing to the high model density. Models with structural and aerodynamic damping coefficients more representative of full scale values should be used for measurements of the level of buffeting.

* Replaces R.A.E. Technical Report No.66160 - A.R.C.28632

CONTENTS

1 INTRODUCTION

A previous Report[1] summarises the fair correlation between buffet boundaries measured on seven small solid models in wind tunnels and corresponding flight buffet boundaries. The present report examines a more difficult problem, the estimation of the level of model buffeting and its extrapolation to a full scale aircraft using appropriate theoretical scaling relationships[2,3]. These relationships involve structural and aerodynamic damping coefficients.

There is no simple expression for the structural damping coefficient, which is determined by the type of model construction and the type of attachment to the supporting sting. (Table 1 shows measured wind-off structural damping coefficients for models B and D of Ref.1.)

The aerodynamic damping coefficient γ varies directly as the density ratio of the free stream/model because

$$\gamma = C_{L\alpha,\ell} \cdot q/M_1 \cdot S_2/2\,\omega_1\, V \qquad (1)$$

where $C_{L\alpha,\ell}$ = first mode generalised lift curve slope for damping component of aerodynamic force owing to wing vibration,

q = kinetic pressure (α free stream density ρ);

M_1 = generalised wing mass for first mode vibration (α model density ρ_m);

S_2 = weighted wing area for first mode vibration;

ω_1 = undamped natural circular frequency for first mode,

and V = velocity.

For the particular example of a wing of constant chord d and constant thickness chord ratio t/d the aerodynamic damping coefficient is

$$\gamma = \tfrac{1}{2} \cdot \rho/\rho_m \cdot V/tf_1 \qquad (2)$$

where the mass/unit span is assumed equal to

$$\rho_m\, dt/2$$

and $C_{L,\alpha} \simeq 2\pi$.

Now although the seven solid models considered previously have approximately the correct frequency parameter (Table 1 Ref.1).

i.e. $$(tf_1/V)_{model} \simeq (tf_1/V)_{aircraft}$$

they cannot have the correct density ratio because the density of the model wing is higher than that of the aircraft and the 3 ft tunnel density is limited to 2x atmospheric density. Hence solid models have low aerodynamic damping coefficients in the 3 ft tunnel, and the structural damping coefficient is likely to predominate, even when the model structural damping coefficient is low and comparable to that of the aircraft.

If the structural damping coefficient predominates over the aerodynamic damping coefficient the variation of the level of buffeting with density is[3]

$$\text{wing-root strain} \propto \rho \qquad (3)$$

as previous limited tests on models A, B, D and E of Ref.1 had suggested. However, if the aerodynamic damping coefficient predominates

$$\text{wing-root strain} \propto \rho^{\frac{1}{2}} \qquad (4)$$

as in some early flight experiments[2].

In the present tests the validity of equation (3) for model D was confirmed (Fig.8) by testing over a wide range of free stream density (4/1). Model D (the Scimitar Mk.1) was selected because the tunnel and flight buffet boundaries are in good agreement at the test Mach number M = 0.50 (Fig.1).

Previous buffeting measurements by Rainey[4], in which the density ratio was varied by testing identical wings made of magnesium, aluminium alloy and steel, appear to satisfy equation (4), even though the structural damping was significant.

2 EXPERIMENTAL DETAILS

2.1 Buffeting measuring equipment

Model D was provided with four active semi-conductor strain gauges wired to add the port and starboard strain signals which eliminated the antisymmetric wing-root strain owing to model rolling. The strain gauge bridge was powered by a 6.3V battery and the signal lead was connected to a

spectrum analyser* which gave a direct voltage reading. This was the second method of measuring buffeting described in Ref.1 and was not available for the previous tests in October 1963. The present tests were made in January 1965. The total rms signals obtained by the two different methods agree quite well (Fig.2). On this steel wing with semi-conductor strain gauges a signal of 100μV corresponds with an rms surface stress of 4 lb/in^2.

2.2 Model D

Model D is shown in Fig.3. It was mounted on a specially manufactured solid sting to reduce sting deflections instead of the six component balance used for the previous tests. Table 1 gives the principal modes of vibration and structural damping coefficients found by a wind off ground resonance test with the model mounted in the tunnel; the frequencies of the port and starboard wings are slightly different. Although both wings are slotted into the fuselage and secured by bolts the wind off structural damping is low and may fall with increasing lift (3.1 below). Table 1 also gives (for subsequent discussion) corresponding modes and frequencies for model B, machined from one piece of dural.

2.3 Test conditions

In these tests the kinetic pressure $q = \frac{1}{2} \rho V^2$ was varied by varying the free stream density at constant Mach number; thus the frequency parameter (tf_1/V) remains constant. The Mach number chosen, M = 0.50 was sufficiently low that unsteadiness in the slotted working section[5] did not effect the wing buffeting. (This was demonstrated in a preliminary experiment 3.1.)

Table 2 shows the Reynolds number variation with density. The tests were not extended to lower densities because the buffet boundary started to alter at $\rho = 0.36$ lb/ft^2 ($R = 0.47 \times 10^6$). Transition fixing bands of carborundum in aluminium paint were attached to the leading edges of the wings, tailplane and fin. This roughness was intended to fix transition at $R = 1.25 \cdot 10^6$ and was not altered as the density varied.

3 RESULTS

3.1 Subtraction of tunnel unsteadiness signal

Previous tests[1] showed that at transonic speeds there was some correlation between the unsteadiness in the slotted working section and the wing buffeting. To minimise this difficulty the present tests were made at a subsonic Mach number, M = 0.50, where the unsteadiness in the slotted working

* A Brüel and Kjaer 2107

section was much reduced. A preliminary test, described below, demonstrated that the remaining unsteadiness did not influence the wing buffeting.

The model was tested first in the closed 3 x 3 ft working section and then the slotted liners were inserted to form a 3 x 2.2 ft working section with higher unsteadiness and the tests repeated. Fig.4(a) shows the variation of the total wing-root strain signal with incidence for both tunnel configurations. The shape of both curves is similar but the unsteadiness signal in the slotted working section at zero incidence is nearly 50% higher than in the closed working section (this is consistent with previous experience in the 3 ft tunnel[5]). If there is no correlation between the wing buffeting and the tunnel unsteadiness then

$$WRS_B = (WRS_T^2 - WRS_o^2)^{\frac{1}{2}} \qquad (5)$$

where WRS_B = wing buffeting signal in absence of tunnel unsteadiness

WRS_T = total wing signal

WRS_o = wing signal owing to tunnel unsteadiness at zero incidence.

Equation (5) correlates both sets of data (Fig.4(b)) and hence may be used to subtract the component of the wing signal owing to tunnel unsteadiness at other stream densities in the slotted working section.*

The small increase in signal between 0° and 6° in Fig.4(b) may come from a small decrease in wing structural damping as observed previously[3] with a model of similar construction.

3.2 Types of flow separations inducing buffeting

Even after applying the correction for tunnel unsteadiness Fig.4(b) still shows a rounding of the curve between $\alpha = 6^\circ$ and 10° which makes it impossible to define buffet onset without drawing intersecting tangential curves through the signal at low incidence (0° to 6°) and high incidence (10.5° to 12.0°). Oil flow runs (Fig.5) showed that the flow was attached over the wing at $\alpha = 5^\circ$. However at $\alpha = 6^\circ$ two small vortices formed on the wing tip outboard of the boundary layer fence and these combined to form a large single vortex as incidence increased to 8°. This vortex induces the mild buffeting between 6° and 8° (c.f. the vortex induced buffeting of Model F, Ref.1, Fig.21). At 10° incidence the flow suddenly separates inboard of the fence and there is

* The high densities required for these tests could only be reached in the slotted working section because of a power limitation.

severe buffeting. The tip buffeting is mild and is not reported in flight; this "two stage" flow separation excites two different vibration modes on the model wing.

3.3 Modes of wing buffeting

The "wind-on" wing vibration modes were found by setting the model at $\alpha = 12^{\circ}$ (2° beyond the severe buffeting onset) and tuning the spectrum analyser. The modes excited at 26, 160, 330, 520 and 760 c/s had all appeared in the ground resonance test. The wing-root strain signal was then measured at each of these tuned frequencies (with 6% bandwidth) over the incidence range from 0° to 12°. Fig.6(a) - (e) shows that only the fundamental wing bending shows any significant variation with incidence and that this mode responds to the tip vortex buffet, as well as the centre section buffet.

Only one mode was excited above 760 c/s. This mode was much higher, at 1800 c/s and was not identified in the ground resonance test; this mode was only excited when the centre section stalled. Fig.6(f).

Both the wing fundamental mode (at $f_1 = 520$ c/s) and the unidentified mode at 1800 c/s were used for the subsequent buffeting investigation.

3.4 Buffeting scaling laws

The variation of buffeting severity with density depends on the relative magnitudes of the structural and aerodynamic damping coefficients[3]. If the structural damping coefficient predominates

$$\text{wing-root strain} \quad \alpha \quad \rho \qquad (3)$$

whereas if the aerodynamic damping coefficient predominates

$$\text{wing-root strain} \quad \alpha \quad \rho^{\frac{1}{2}} \quad . \qquad (4)$$

Fig.7 shows the measured variation of wing-root strain signal with incidence and density for both modes of vibration. Figs.8 and 9 show the same data, corrected for tunnel unsteadiness, and compared by using both equations (3) and (4). (The scales of Figs.8 and 9 have been adjusted so that the points for the highest density $\rho = 0.135$ lb/ft^3 are identical.) Careful examination of Fig.8 suggests that equation (3) is valid for the fundamental mode at 520 c/s and hence that the structural damping coefficient predominates. The measured wind-off structural damping coefficient is low ($g/2 = 0.010$) but

the estimated* aerodynamic damping coefficient is also low ($\gamma = 0.007$) even at $\rho = 0.136$ lb/ft^3, the highest free stream density, because the model density is high.

The ground resonance test of model B revealed a similar situation. Model B is machined from one piece of light alloy and the measured wind-off structural damping coefficient of the wing fundamental mode at 287 c/s is low ($g/2 = 0.028$). However the estimated aerodynamic damping coefficient at the previous maximum test density $\rho = 0.066$ lb/ft^3 is low ($\gamma = 0.016$) despite the low model density. Hence the structural damping coefficient would probably predominate even on this model, which apparently represents the limit of good solid construction. This was certainly the implication of some previous tests of Model B over a reduced density range, when equation (3) provided the best fit of the limited data.

Thus while buffet onset can be measured on a solid wind tunnel model (provided it has about the right reduced wing frequency) the level of buffeting can only be investigated on a special model which has the correct reduced frequency and density and hence the correct aerodynamic damping coefficient i.e. a true aeroelastic model of the aircraft. In addition to having the correct aerodynamic damping coefficient an aeroelastic model has similar mass and stiffness distributions which simplifies the application of the buffeting scaling relationships. If the model is made of the same material as the aircraft, (as high speed flutter models often are), the model stress is equal to that on the aircraft at the corresponding point[6]. Buffeting measurements on two aeroelastic models of slender wing aircraft are included in another report[7].

Returning to Model D, Fig.9 suggests that the structural damping coefficient may also predominate for the unidentified mode but the structural damping coefficient was not measured and the aerodynamic damping coefficient could not be estimated because the deformation mode was unknown.

4 CONCLUSIONS

The variation of unsteady wing-root strain signal with free stream density produced by wing buffeting on a small solid model of the Scimitar aircraft shows that the structural damping coefficient predominates over the aerodynamic damping coefficient (Fig.8). This is because the aerodynamic damping coefficient is low owing to the high model density even though the

---

* Equation (2) was used to make this approximate estimate.

structural damping coefficient is low. Hence although solid wind tunnel models are adequate for determining buffet boundaries (an important practical problem), aeroelastic models with the correct aerodynamic and structural damping coefficients are necessary for measurements of the level of buffeting (3.4).

Preliminary experiments showed that on this model unsteadiness at subsonic speeds in the slotted working section did not influence the wing buffeting (3.1), and that the two different types of flow separation on the wing excited two different modes of wing response (3.2 and 3.3).

Acknowledgement

The author is grateful to Mr. L. Martin of the Dynamic Test Section, B.A.C., Filton for the measurements given in Table 1.

Table 1

Wind off structural characteristics

Mode	Model D		Model B	
	Frequency C/S	Damping $g/2 = C/C_{crit}$	Frequency C/S	Damping $g/2 = C/C_{crit}$
Sting fundamental	28	0.005	33	0.003
Model roll	150	0.002	135	0.012
Antisymmetric wing bending	335	0.007	154	0.007
Wing fundamental	535 (port) 518 (starboard)	0.010	287	0.028
First overtone wing bending	755	0.012	379	0.008
Second overtone bending	-	-	630	0.013

Table 2

Test conditions M = 0.50

Working section density lb/ft^3	Reynolds number $(\bar{d})$ $\times 10^{-6}$
0.036	0.47
0.057	0.73
0.066	0.85
0.098	1.25
0.135	1.72

SYMBOLS

b	wing span
c	velocity damping of system
C_{crit}	critical damping required to reduce the free motion of the system from periodic to aperiodic
$C_{L\alpha,\ell}$	first mode generalised lift curve slope for damping component of aerodynamic force owing to wing vibration
d	wing chord
$\bar{d}$	average chord
f_1	wing fundamental frequency (c/s)
$g/2$	structural damping coefficient (% critical) C/C_{crit}
M	Mach number
M_1	generalised wing mass for first mode vibration
q	kinetic pressure $\frac{1}{2} \rho V^2$
R	Reynolds number (based on average chord $\bar{d}$)
WRS	wing-root strain
V	velocity (ft/s)
S_2	weighted wing area for first-mode bending
t	wing thickness
α	incidence (^{o})
γ	aerodynamic damping coefficient (% critical) $= C_{L\alpha,\ell} \cdot q\, S_2/2\, M_1\, \omega_1\, V$
ρ	free stream density
ρ_m	model density
ω_1	undamped natural circular frequency for first mode $= 2\pi f_1$

REFERENCES

No.	Author	Title, etc.
1	D. G. Mabey	Comparison of seven wing buffet boundaries measured in wind tunnels and in flight. A.R.C. C.P.840, September 1964
2	W. B. Huston	A study of the correlation between flight and wind tunnel buffet loads. AGARD Report 111, May 1957
3	D. D. Davis, Jr.	Buffet tests of an attack-airplane model with emphasis on analysis of data from wind-tunnel tests. NACA RM L57H13, February 1958
4	A. G. Rainey T. A. Byrdsong	An examination of methods of buffeting analysis based on experiments with wings of varying stiffness. NASA TN D 3, August 1959
5	D. G. Mabey	Unpublished Min. Tech. Report.
6	W. H. Melbourne	Aerodynamic investigation of the wind loads on a cylindrical lighthouse. A.R.L. (Australia) Note A.224
7	D. G. Mabey	Measurements of buffeting on slender wing models. A.R.C. C.P.917, March 1966

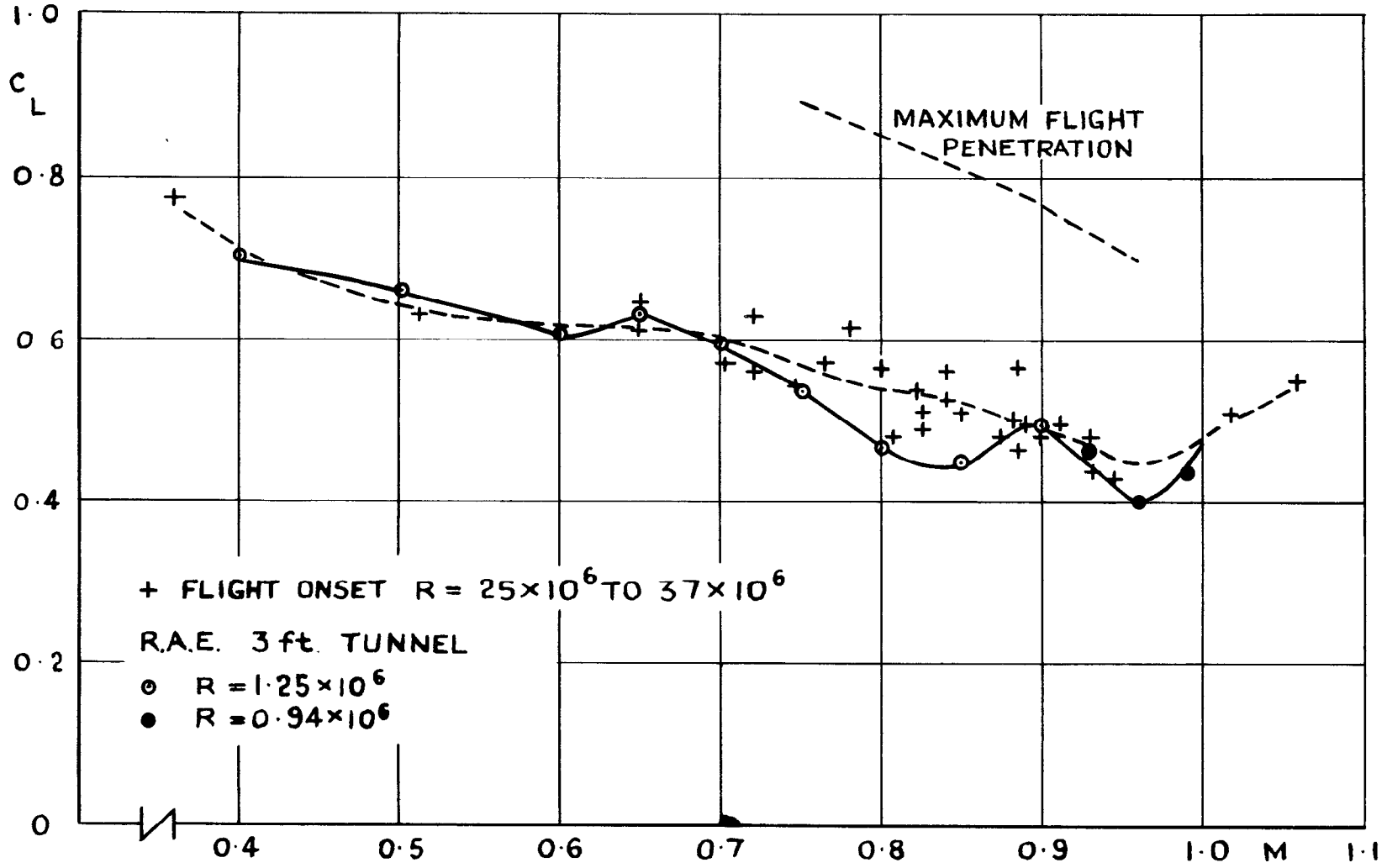

FIG.1 MODEL D-COMPARISON OF TUNNEL & FLIGHT BUFFET BOUNDARIES.

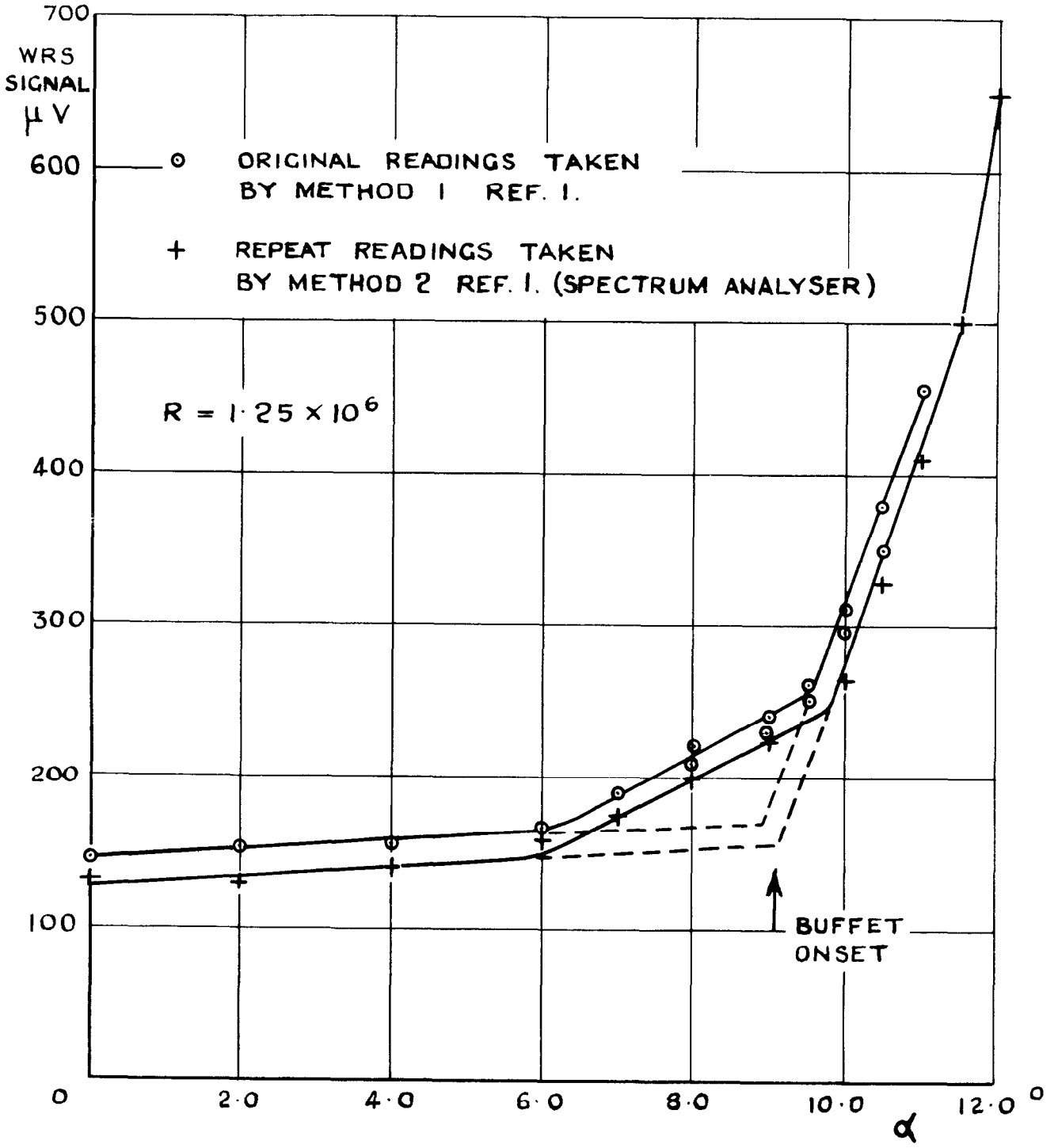

FIG 2 MODEL D. COMPARISON OF TWO METHODS OF MEASURING WING BUFFETING M = 0·50

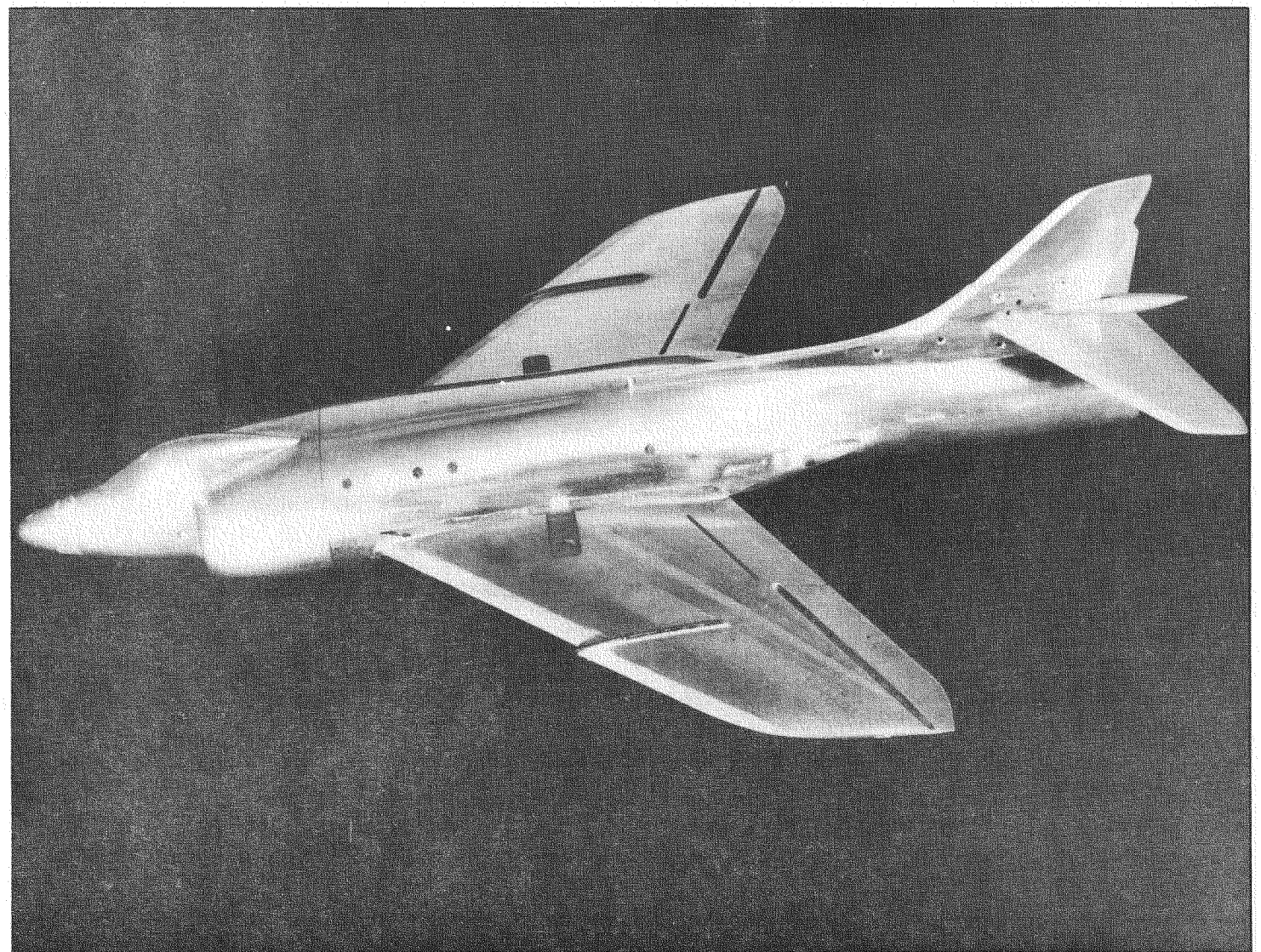

Fig.3 1/50th. scale Scimitar model - model D (Ref. 1)

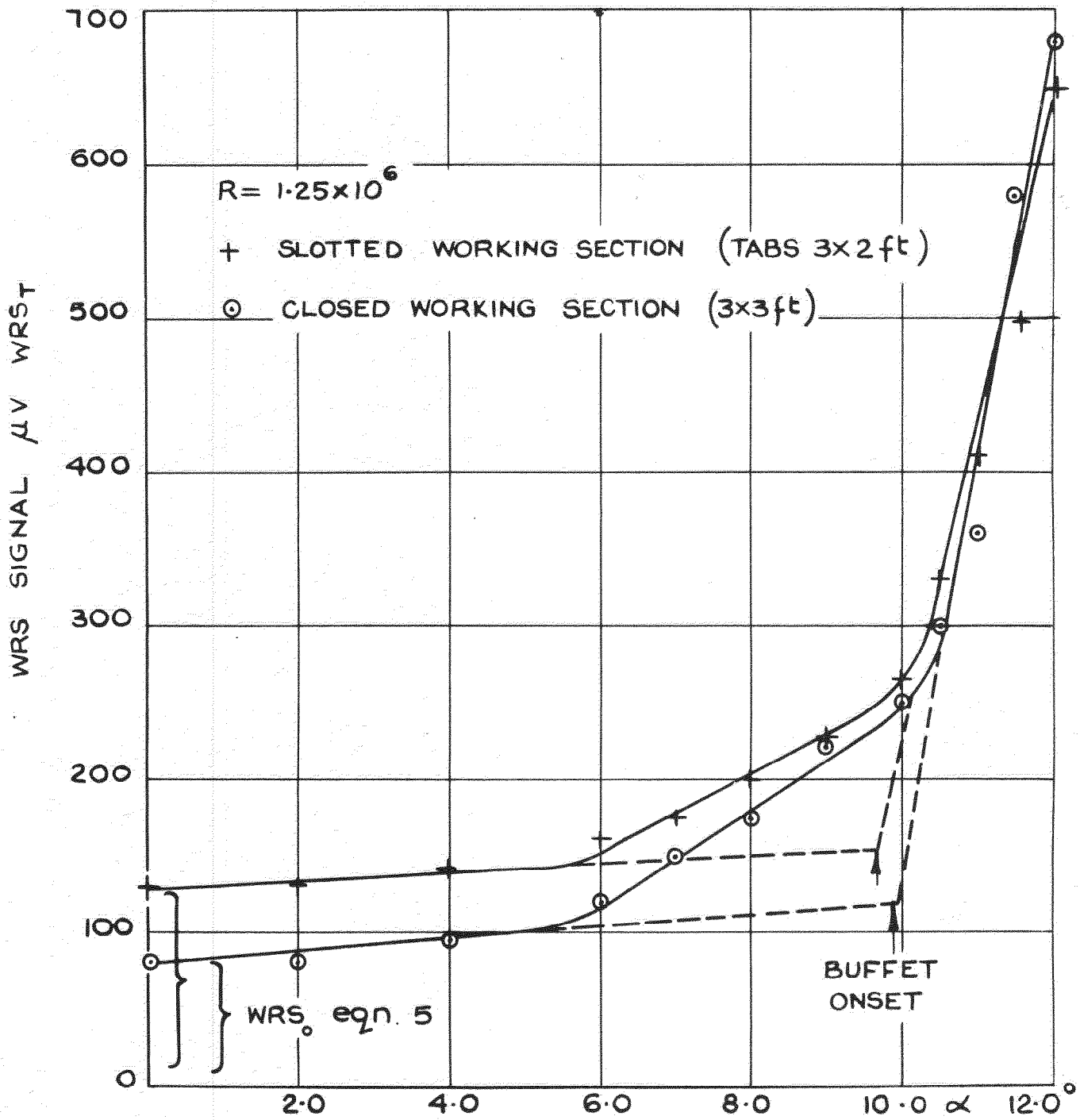

FIG. 4 (a) UNCORRECTED FOR TUNNEL UNSTEADINESS

FIG. 4 MODEL D-VARIATION OF WING-ROOT STRAIN SIGNAL WITH INCIDENCE IN SLOTTED AND CLOSED WORKING SECTIONS M=0.50

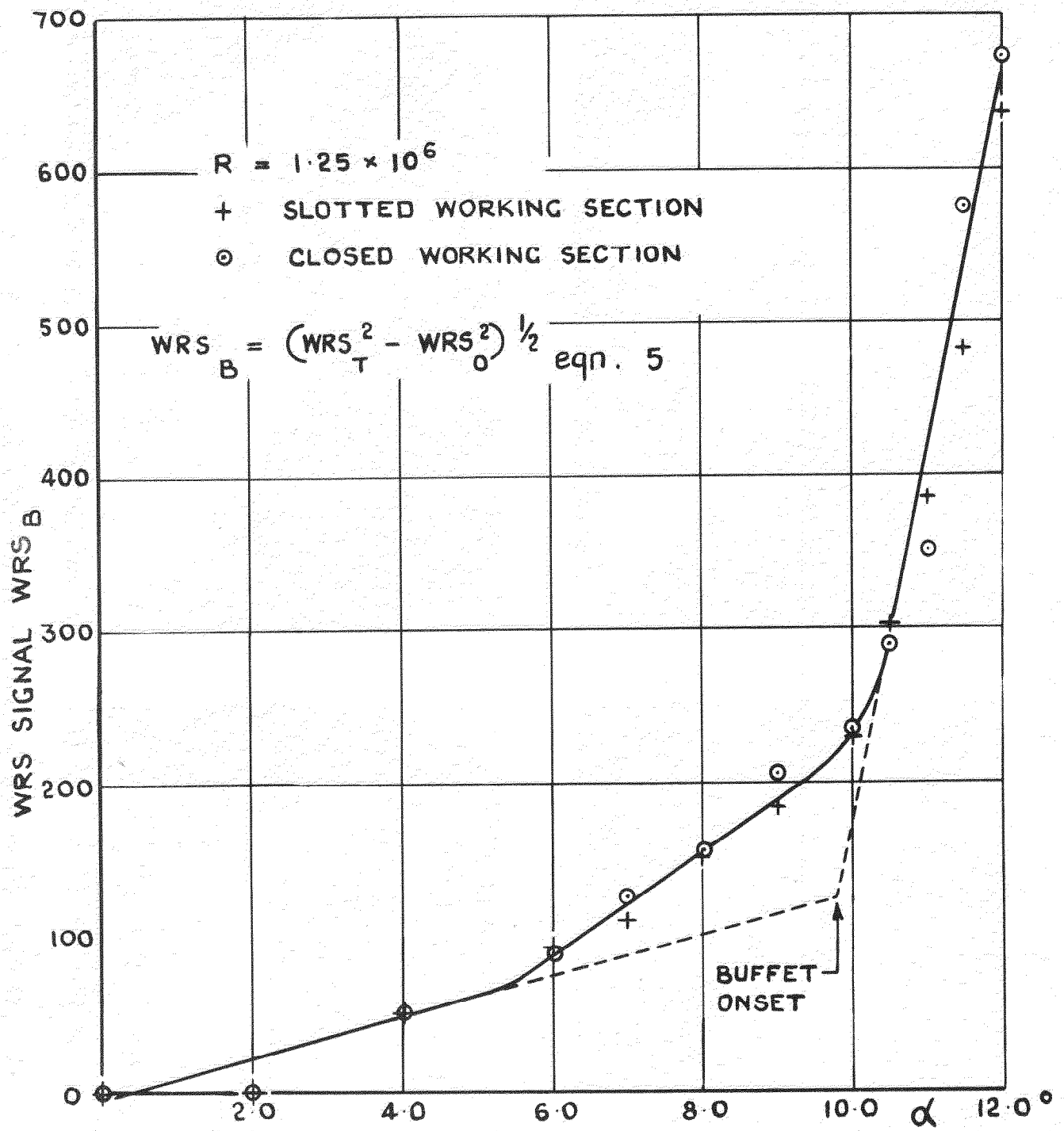

FIG. 4 (b) CORRECTED FOR TUNNEL UNSTEADINESS.

FIG. 4 (CONCLD).

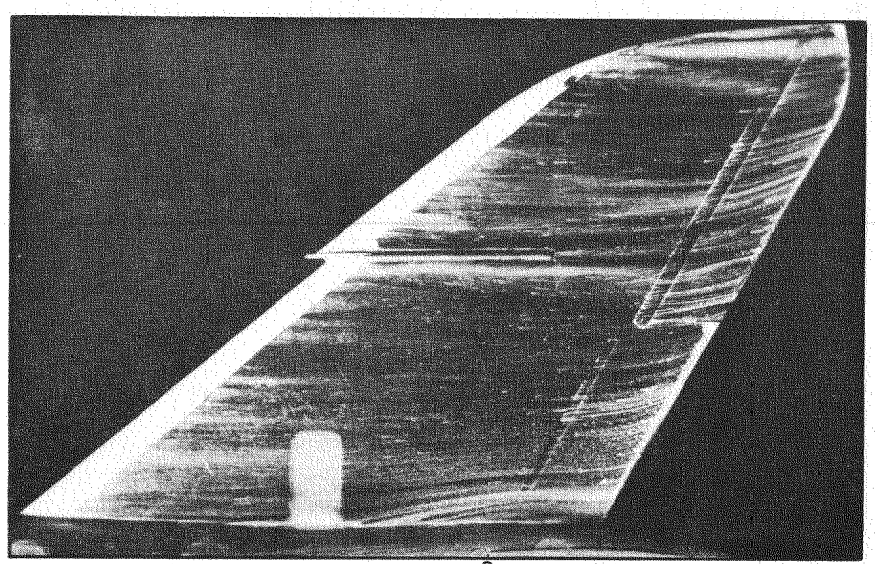

$\alpha = 5°$

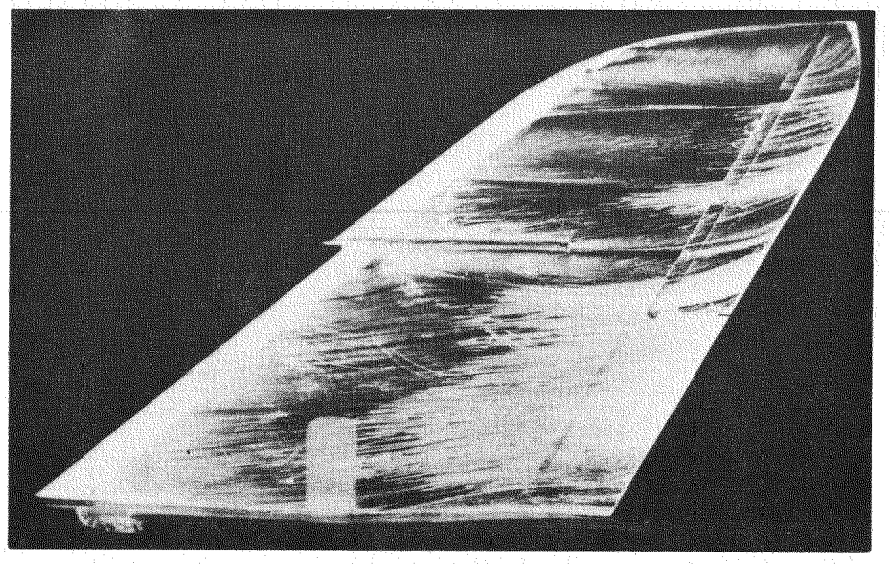

$\alpha = 6°$

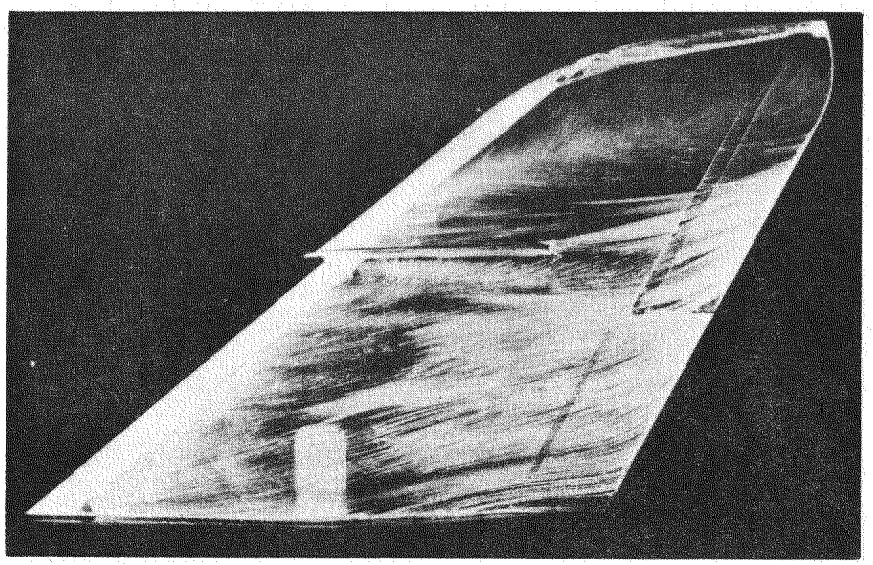

$\alpha = 8°$

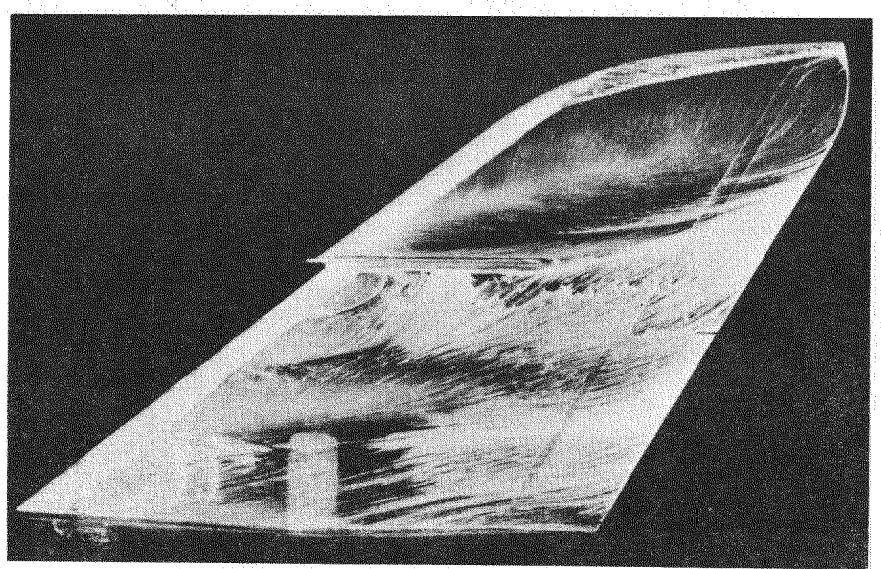

$\alpha = 10°$

Fig.5. Wing D oil flow photographs near buffet onset M=0.50.

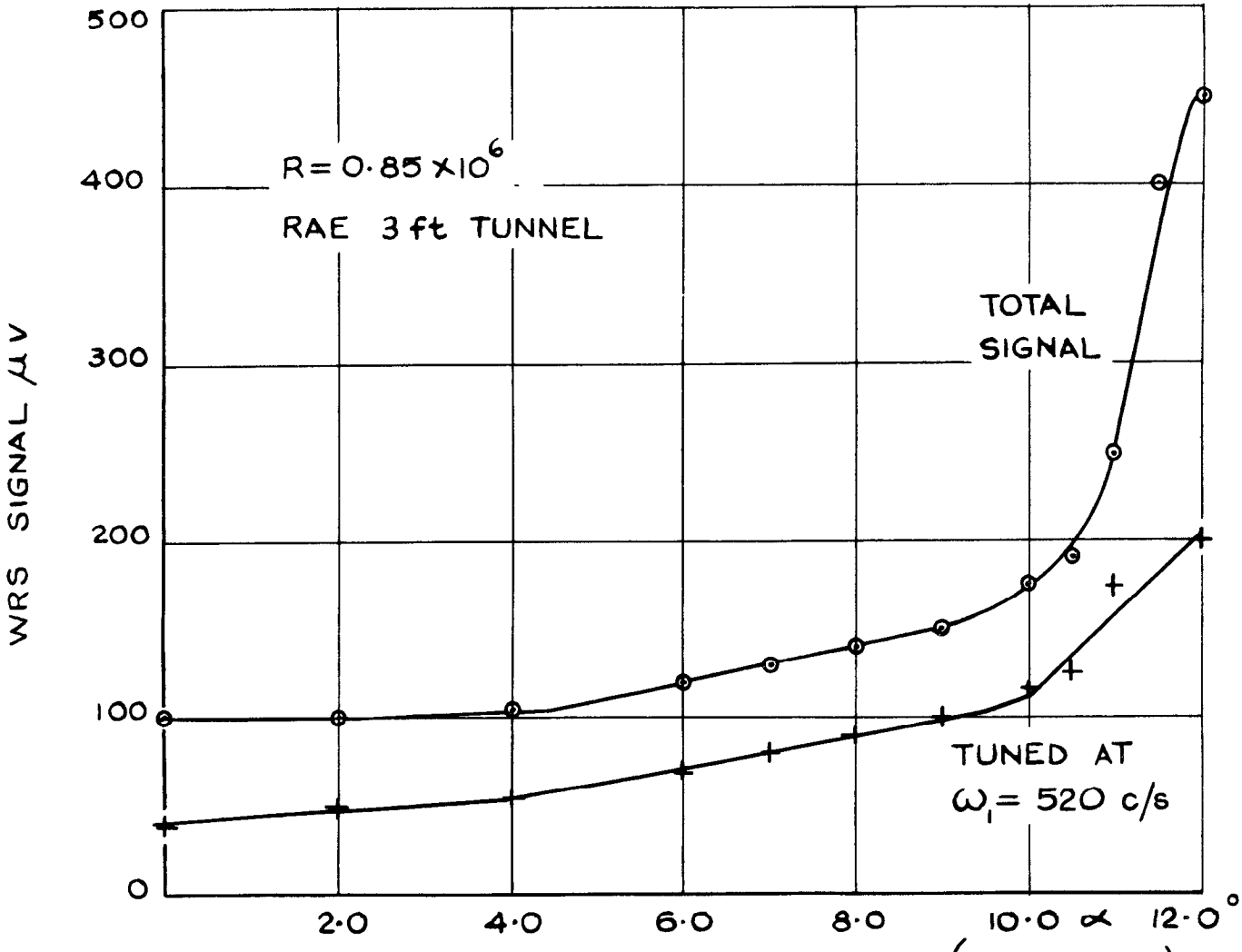

FIG. 6(a) TOTAL SIGNAL AND WING FUNDAMENTAL (ω_1 = 520 c/s)

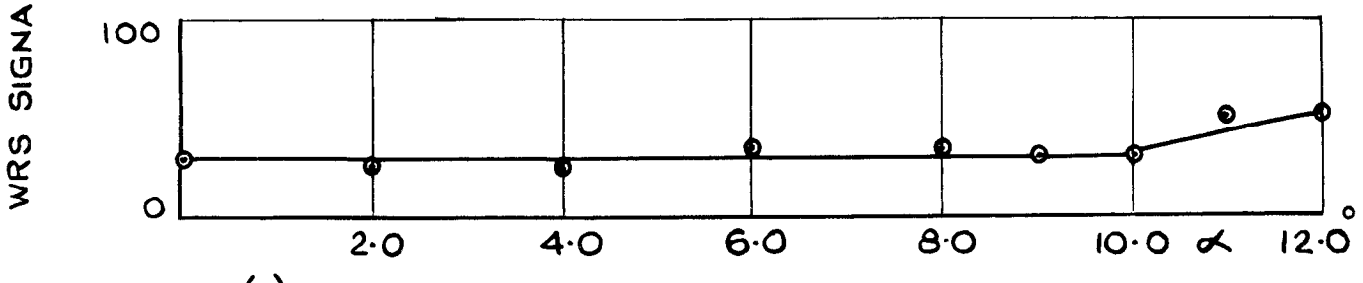

FIG. 6(b) STING FUNDAMENTAL FREQUENCY = 26 c/s

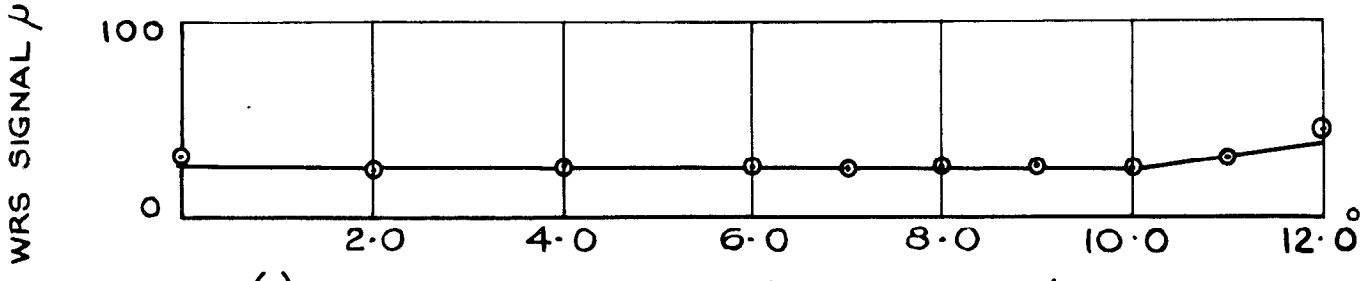

FIG. 6(c) MODEL ROLLING FREQUENCY = 160 c/s

FIG. 6 MODEL D–COMPONENTS OF WING–ROOT STRAIN SIGNAL M=0·50

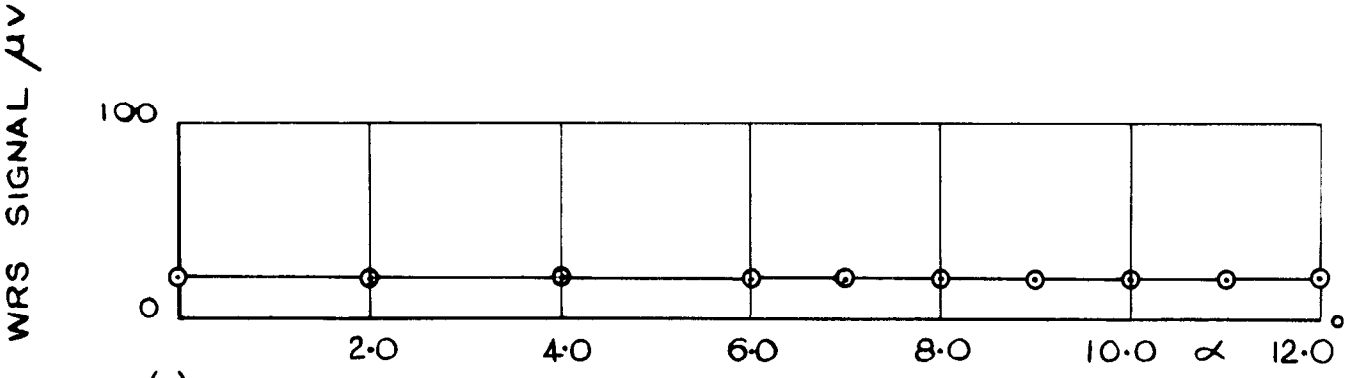

FIG. 6 (d) ANTISYMMETRIC WING BENDING FREQUENCY = 330 c/s

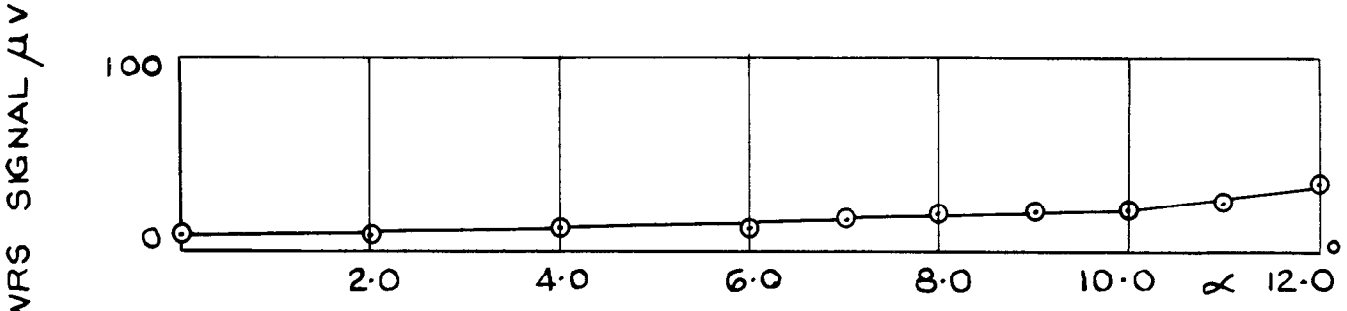

FIG. 6 (e) OVERTONE WING BENDING FREQUENCY = 760 c/s

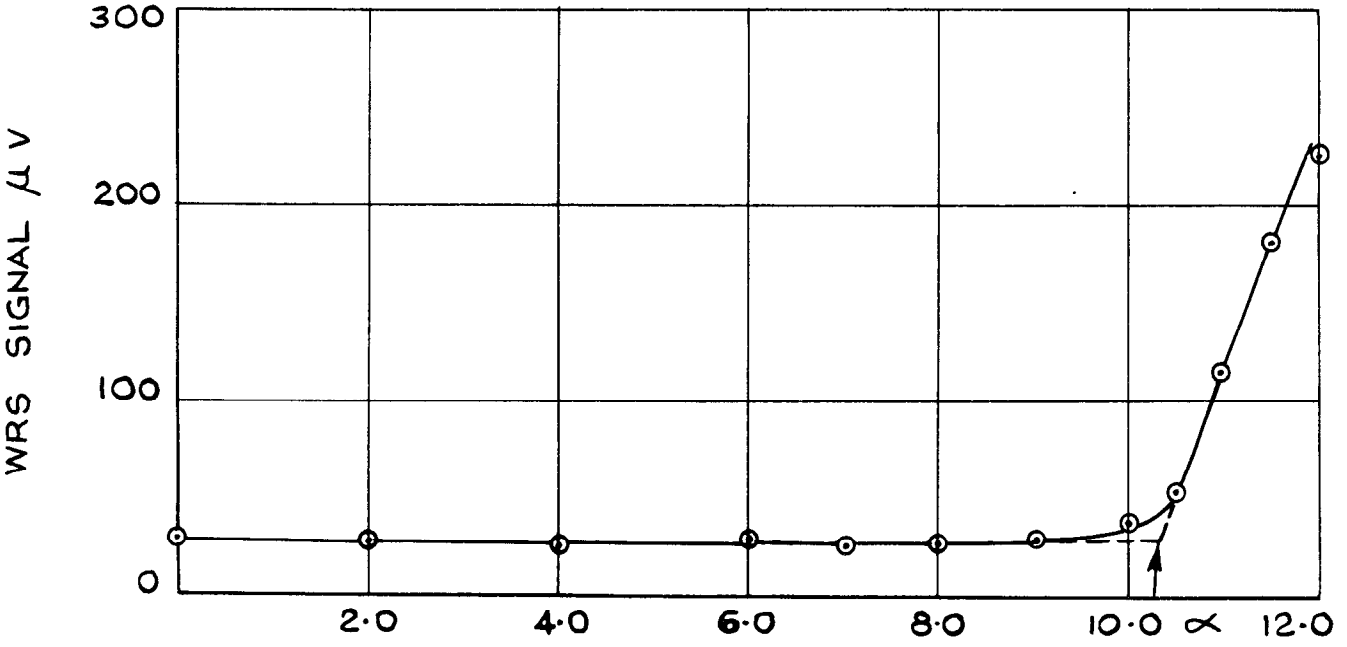

FIG. 6 (f) UNIDENTIFIED MODE; FREQUENCY = 1,800 c/s

FIG. 6 (CONCLD)

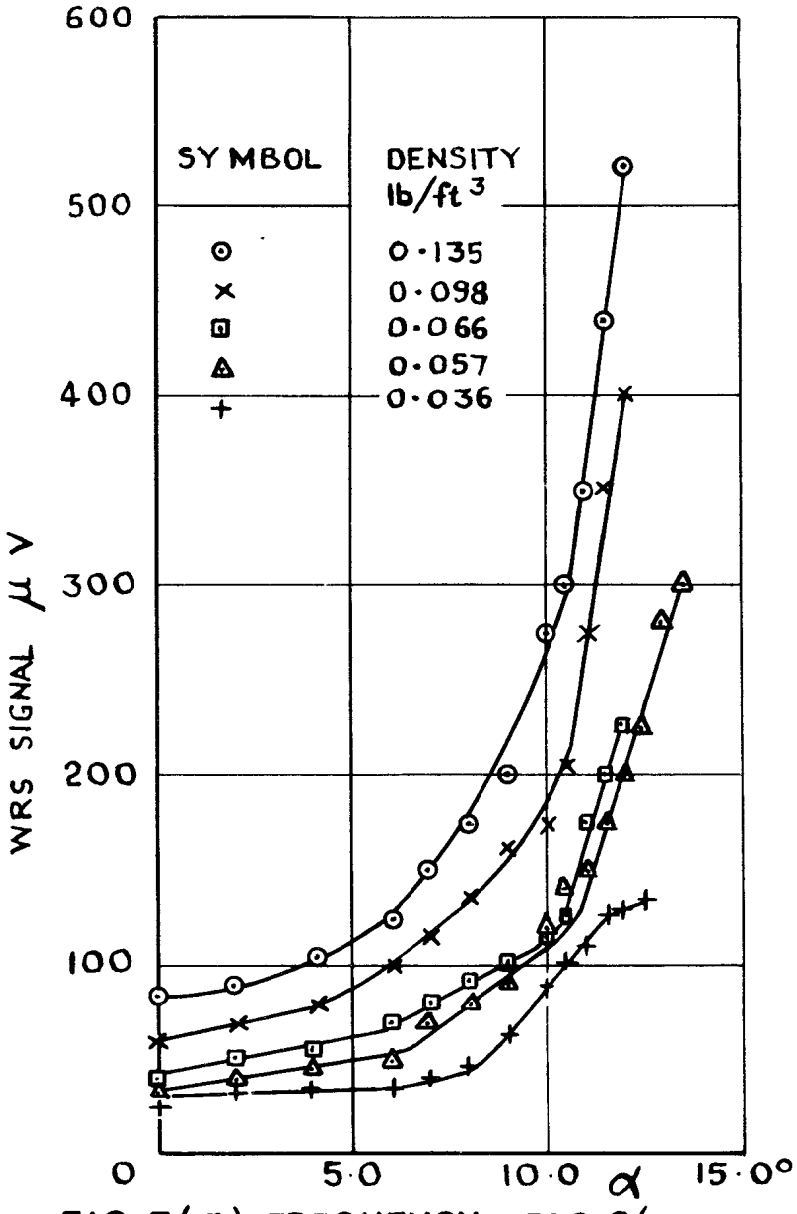

FIG. 7 (a) FREQUENCY = 520 c/s.

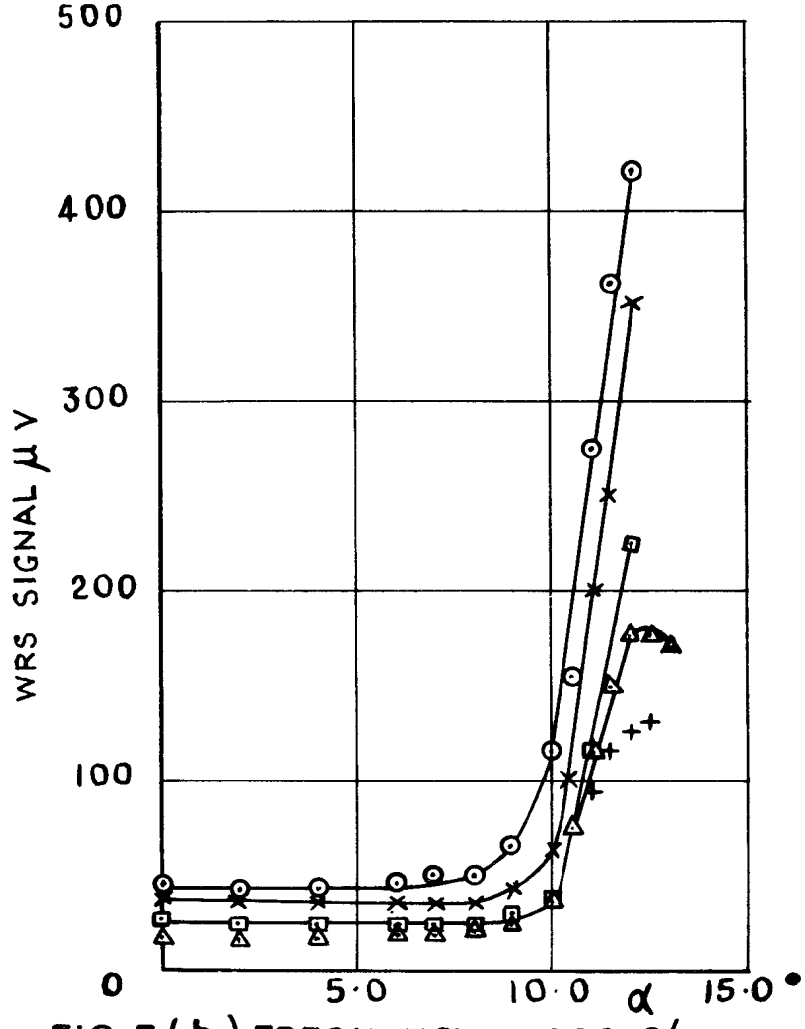

FIG. 7 (b) FREQUENCY = 1,880 c/s.

FIG. 7 MODEL D VARIATION OF WING-ROOT STRAIN SIGNAL WITH INCIDENCE AND DENSITY M=0·50

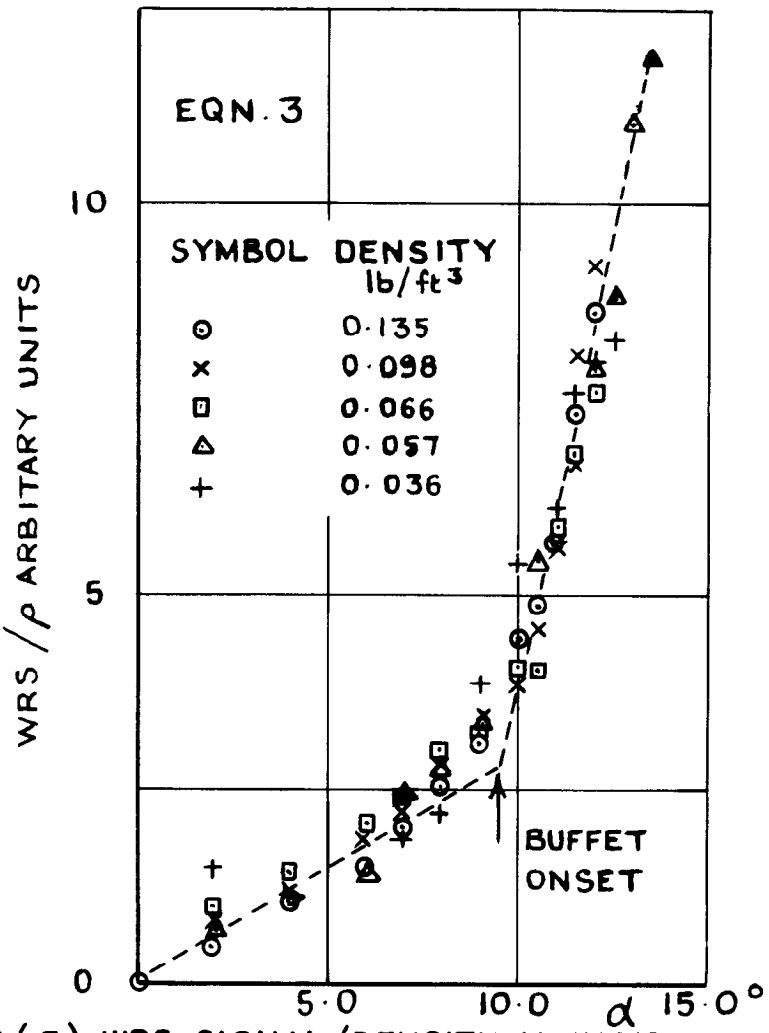

FIG.8 (a) WRS SIGNAL/DENSITY V INCIDENCE

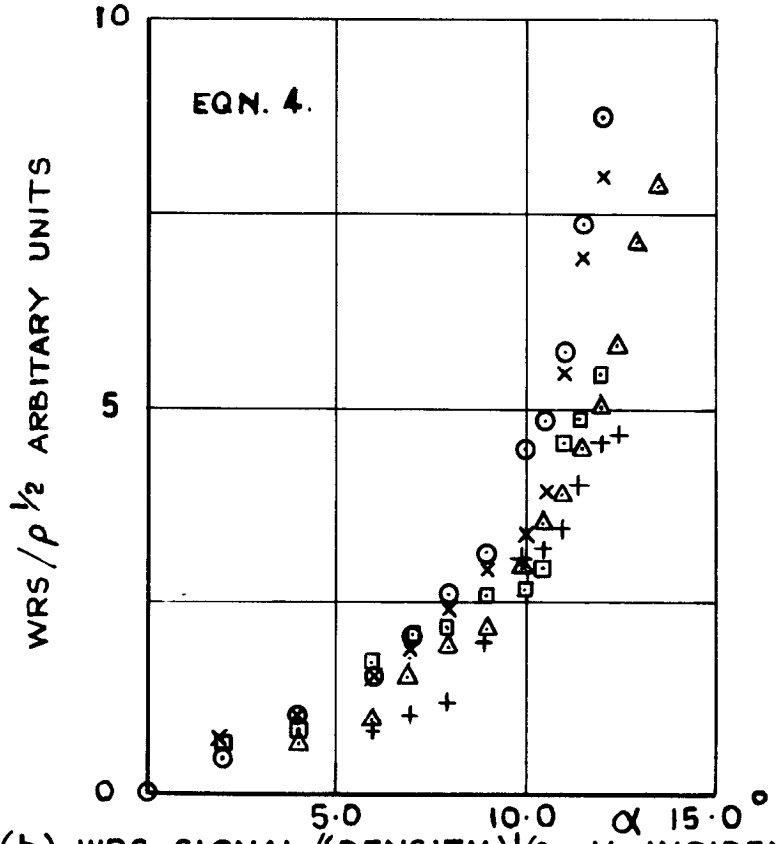

FIG.8 (b) WRS SIGNAL/(DENSITY)$^{1/2}$ V INCIDENCE

FIG.8 MODEL D COMPARISON OF BUFFETING SCALING LAWS FREQUENCY=520 c/s M=0·50

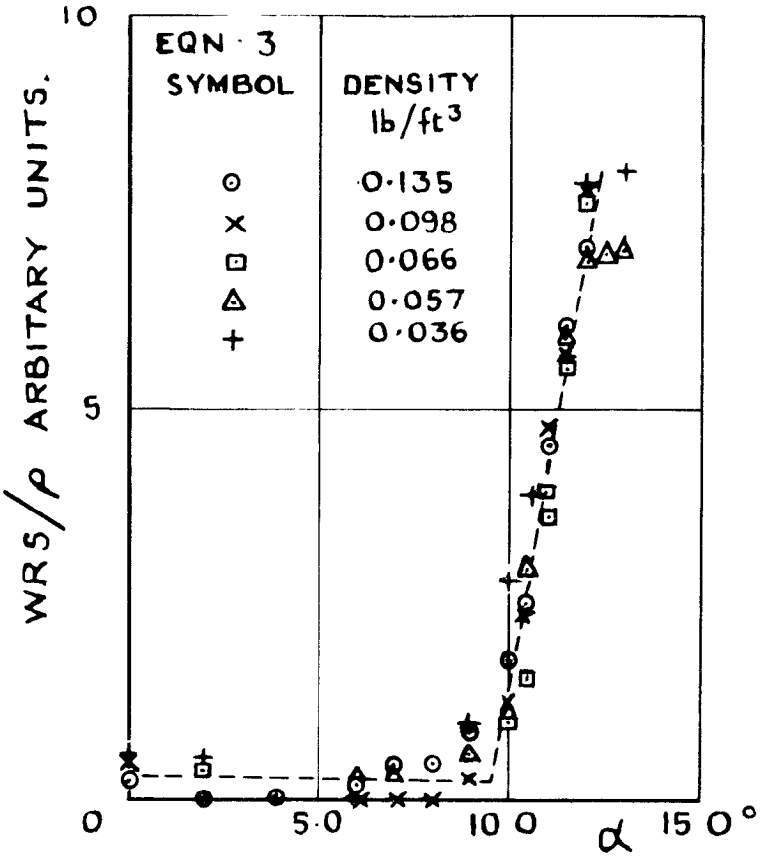

FIG. 9 (a) WRS SIGNAL/DENSITY V INCIDENCE

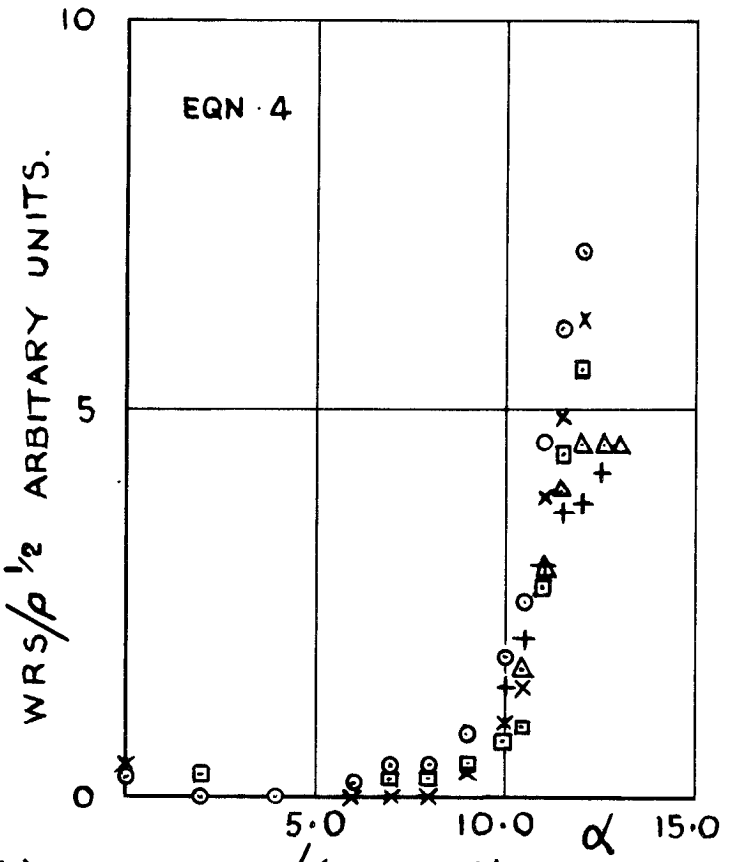

FIG. 9 (b) WRS SIGNAL / (DENSITY)½ V INCIDENCE.

FIG. 9 MODEL D COMPARISON OF BUFFETING SCALING LAWS. FREQUENCY = 1,880 c/s M=0·50

Printed in England for Her Majesty's Stationery Office by the Royal Aircraft Establishment, Farnborough. Dd.129528 K.4.

A.R.C. C.P. No.954
May 1966

533.6.013.43 :
533.693

Mabey, D. G.

MEASUREMENTS OF WING BUFFETING ON A SCIMITAR MODEL

Measurements of unsteady wing-root strain were made on a small solid model of the Scimitar Mk.1 aircraft to investigate the buffeting scaling relationships. The wing-root strain measurements covered an incidence range from 0° to 13° at a Mach number of 0.50 and a wide range of stream density.

The derived buffeting scaling relationships show that the damping of the wing buffeting is predominantly structural (even though the structural damping coefficient on this model is low) because the aerodynamic damping coefficient is low owing to the high model density. Models with structural and aerodynamic damping coefficients more representative of full scale values should be used for measurements of the level of buffeting.

A.R.C. C.P. No.954
May 1966

533.6.013.43 :
533.693

Mabey, D. G.

MEASUREMENTS OF WING BUFFETING ON A SCIMITAR MODEL

Measurements of unsteady wing-root strain were made on a small solid model of the Scimitar Mk.1 aircraft to investigate the buffeting scaling relationships. The wing-root strain measurements covered an incidence range from 0° to 13° at a Mach number of 0.50 and a wide range of stream density.

The derived buffeting scaling relationships show that the damping of the wing buffeting is predominantly structural (even though the structural damping coefficient on this model is low) because the aerodynamic damping coefficient is low owing to the high model density. Models with structural and aerodynamic damping coefficients more representative of full scale values should be used for measurements of the level of buffeting.

A.R.C. C.P. No.954
May 1966

533.6.013.43 :
533.693

Mabey, D. G.

MEASUREMENTS OF WING BUFFETING ON A SCIMITAR MODEL

Measurements of unsteady wing-root strain were made on a small solid model of the Scimitar Mk.1 aircraft to investigate the buffeting scaling relationships. The wing-root strain measurements covered an incidence range from 0° to 13° at a Mach number of 0.50 and a wide range of stream density.

The derived buffeting scaling relationships show that the damping of the wing buffeting is predominantly structural (even though the structural damping coefficient on this model is low) because the aerodynamic damping coefficient is low owing to the high model density. Models with structural and aerodynamic damping coefficients more representative of full scale values should be used for measurements of the level of buffeting.

DETACHABLE ABSTRACT CARDS

Published by
HER MAJESTY'S STATIONERY OFFICE

To be purchased from
49 High Holborn, London W.C.1
423 Oxford Street, London W.1
13A Castle Street, Edinburgh 2
109 St. Mary Street, Cardiff
Brazennose Street, Manchester 2
50 Fairfax Street, Bristol 1
35 Smallbrook, Ringway, Birmingham 5
7-11 Linenhall Street, Belfast 2
or through any bookseller

C.P. No. 954

S.O. CODE No. 23-9017-54